Received 30 April 2019; revised 26 July 2019; accepted 9 August 2019. Date of publication 19 August 2019; date of current version 11 December 2019.

Digital Object Identifier 10.1109/JPETS.2019.2935703

Sampling-Based Model Predictive Control of PV-Integrated Energy Storage System Considering Power Generation Forecast and Real-Time Price

JUAN OSPINA[1,3] (Student Member, IEEE), NIKHIL GUPTA[2] (Member, IEEE), ALVI NEWAZ[1,3] (Student Member, IEEE), MARIO HARPER[3,4], M. OMAR FARUQUE[1,3] (Senior Member, IEEE), EMMANUEL G. COLLINS, JR.[4] (Senior Member, IEEE), RICK MEEKER[5] (Member, IEEE), AND GWEN LOFMAN[3]

[1]Center for Advanced Power Systems, Tallahassee, FL 32310 USA
[2]Halodi Robotics, 1599 Moss, Norway
[3]Florida State University, Tallahassee, FL 32310 USA
[4]Center for Intelligent Systems, Control, and Robotics (CISCOR), Tallahassee, FL 32310 USA
[5]Nhu Energy, Tallahassee, FL 32310 USA

CORRESPONDING AUTHOR: M. O. FARUQUE (faruque@caps.fsu.edu)

This work was supported in part by the U.S. Department of Energy, Office of Science SBIR/STTR Program and Office of Energy Efficiency and Renewable Energy, SunShot Program, under Award DE-SC0015936.

ABSTRACT This paper proposes a novel control solution designed to solve the local and grid-connected distributed energy resources (DERs) management problem by developing a generalizable framework capable of controlling DERs based on forecasted values and real-time energy prices. The proposed model uses sampling-based model predictive control (SBMPC), together with the real-time price of energy and forecasts of PV and load power, to allocate the dispatch of the available distributed energy resources (DERs) while minimizing the overall cost. The strategy developed aims to find the ideal combination of solar, grid, and energy storage (ES) power with the objective of minimizing the total cost of energy of the entire system. Both offline and controller hardware-in-the-loop (CHIL) results are presented for a 7-day test case scenario and compared with two manual base test cases and four baseline optimization algorithms (Genetic Algorithm (GA), Particle Swarm Optimization (PSO), Quadratic Programming interior-point method (QP-IP), and Sequential Quadratic Programming (SQP)) designed to solve the optimization problem considering the current status of the system and also its future states. The proposed model uses a 24-hour prediction horizon with a 15-minute control horizon. The results demonstrate substantial cost and execution time savings when compared to the other baseline control algorithms.

INDEX TERMS Controller Hardware-in-the-Loop (CHIL), distributed energy resources (DER), distributed generation (DG), distributed storage (DS), energy management, real-time pricing, model predictive control (MPC).

I. INTRODUCTION

AN unprecedented growth of DERs, especially PV and wind, has driven the decentralization of power systems and the increase in deployment of distributed generation (DG) and distributed storage (DS) systems by both utility companies and consumers. Progressively, energy storage systems are becoming more competitive, and companies are starting to heavily invest in the development of lithium-ion batteries, thermal storage, and other types of DS systems to decrease energy costs and stabilize the distribution system.

DG and DS systems have the potential of becoming the cornerstone of the future smart grid. Nonetheless, these systems are still not ready for a harmonious integration to the grid due to their lack of proper control and intermittent nature [1]. In the US, most of the DG and DS systems are being deployed under two basic operating principles:

1) to help in the reduction of metered load through net metering programs, and 2) to sell real power generation to utility companies through power purchase agreements (PPAs). These unsophisticated energy transaction methods limit the optimal utilization of these systems. That is why, in order to maximize the solar penetration and effective utilization of available resources, DERs need to have more sophisticated control approaches that dynamically leverage all the resources available to the system while serving the load in an economical, reliable, and safe way. Such optimal control of the energy resources will translate into direct benefits to both utility companies and regular consumers.

Due to the intermittent characteristics and constraints present in some DER systems, such as solar and wind, optimal energy management has become a challenging optimization problem tackled by many researchers. The most common methods found in the literature are linear programming (LP, MILP) models, genetic algorithms (GA), game theory approaches, particle swarm optimization (PSO), model predictive control (MPC), and other metaheuristic methods such as ant colony optimization (ACO) and crow-search algorithms (CSA), among others. In [2], [3], researchers use mixed-integer linear programming approaches to find the optimal scheduled use of energy storage units together with PV and wind generation using current load demand conditions and optimal power dispatch. Most of these approaches consider only the current state of the system to perform dispatch optimization. However, similar methods also exist where the system is extended to consider future states in order to minimize the overall cost of the system operation. One example is the model presented in [4], where authors propose a model solved using MILP for optimizing multiple DERs and other residential appliances via stochastic optimization and robust optimization based on a demand response program. Another similar approach is presented in [5], where authors formulate the energy scheduling problem of a microgrid system as a stochastic optimization solved using standard convex quadratic programming solvers. In [6], authors propose an online energy management system (EMS) for a hybrid microgrid that contains renewable sources such as PV and wind together with battery storage and variable speed diesel generators. Here, authors propose an EMS that consists of a two-level optimization algorithm where the first level is a rolling optimization, and the second level corresponds to an intrasample correction. In the rolling optimization, DERs are scheduled based on the forecasted information and an MPC approach, while on the intrasample correction, a feedback correction adjusts the schedule based on the errors. Authors formulate the optimization problem as a MILP framework with two objectives: 1) minimize total operating costs, and 2) minimize pollutant gas emissions. Similarly, in [7], authors propose a generic and adaptable energy management system, implemented in an online scheme, designed to minimize the operating costs of the microgrid and reduce the load disconnections. The model claims to be a generic architecture that allows the interaction of measured values together with forecasting and optimization modules. The constrained optimization problem presented here is solved using the CPLEX solver. The energy management system proposed in this paper is tested under different conditions, such as grid-connected and islanded modes. A similar approach is taken in [8] and [9], where researchers propose two-layer (two-stage) optimization approaches designed to solve MINLP formulations of the EM problem of grid-connected microgrids and hybrid ES systems respectively. In [8], authors use a Lyapunov optimization method while in [9], researchers use the IPOPT and Gurobi solvers integrated with MATLAB.

In [10], [11], authors use GA models for solving a mixed-integer nonlinear programming problem of a microgrid system taking into account the current state of the system, cost of emissions, operating costs, and maintenance costs of diesel generators, PV and batteries. Researchers in [12] develop a genetic algorithm (GA) approach to solve the planning problem of an energy management system and a distributed energy storage planning model based on a game-theoretic approach. Both approaches are designed to solve the demand-side management formulations using different approaches. For instance, The GA solves the distributed EM problem using a heuristic approach while the game-theoretical energy management scheme obtains the Nash equilibrium by using the proximal decomposition algorithm. Another distributed approach is presented in [13], where researchers propose a distributed robust energy management scheme designed to control multiple interconnected microgrids (MGs). The objective of the model presented is the optimization of the total operational cost of 4 microgrids tested, where real-time energy trading is available between all neighboring microgrids and the main grid. Authors use an algorithm called DAROSA, derived from the ADMM algorithm, to solve the formulated problem. This problem considers uncertainties such as renewable generation, load consumption, and buy/sell prices coming from the grid. PSO is another well-known heuristic method widely used to solve the energy management problem of a microgrid system. In [14], [15], researchers present economic dispatch and power management solutions for stand-alone microgrids with wind turbines, microturbines, and ES systems. Other new metaheuristic methods have also been proposed for power and energy management of microgrid systems, such as ACO in [16] and the crow-search algorithm in [17], [18]. The results of these heuristic methods are highly dependent on the initial guesses and can be very time-consuming for complex optimization problems with a high number of decision variables.

Several model predictive control (MPC) models have also been proposed for managing ES in a microgrid setting [19], [20] or for power regulation applications in islanded AC/DC microgrids [21]. Similarly, off-line day-ahead stochastic planning/scheduling models have also been proposed in the literature. In these models, the energy management solution is formulated as a stochastic

problem based on scenarios generated by Monte Carlo simulations [22], [23]. These solutions have the disadvantage of being unable to react to real-time fluctuations and being very computationally intensive due to the number of scenarios that must be simulated to achieve an optimal solution. The paper presented in [24] tries to address this difficulty by proposing and studying the performance of a two-step online energy management strategy for a grid-tie microgrid that considers the efficiency of energy storage systems and real-time changes in forecasts. In this case, authors use a nonlinear programming with discontinuous derivatives (DNLP) solver to obtain a cost-efficient energy management solution for a grid-tie microgrid with a battery energy storage system (BESS). As mentioned, the EMS proposed is a two-step energy management strategy where the first step focuses on the scheduling of the available DERs and the second step aims to balance the power flow and reduce the impacts of the forecasting errors.

Contrasting from the papers examined, the solution proposed in this paper provides a different approach to solve the online energy management (EM) scheduling problem using a graph-search approach that takes into account the current and future status of the system to find the optimal planned path solutions that minimize the cost of using the available DER. This paper presents an improved and expanded version of the model presented in [25]. More specifically, this paper presents the following research contributions:

1) A novel control solution that uses Sampling-Based Model Predictive Control (SBMPC) to allocate distributed energy resources (DER) based on the current and future forecasted states of the system.
2) A cost-effective control solution that solves the energy management problem using a graph-search approach that provides a different way for computing the 'optimal' control actions of the system. The proposed method uses a rolling receding horizon approach suitable to handle forecasting errors by adjusting the real-time control actions based on a new search performed at every time-step.
3) A control solution that exploits the use of sampling by discretizing the solution space of the system while taking into account all system constraints. The input-sampling procedure reduces the computational complexity and time needed to solve the nonlinear problem. In essence, this method offers a more straightforward and competitive way of adjusting the trade-off between energy costs and computational cost via input-sampling parameters.
4) A detailed comparison with other competitive models where the EM problem is formulated as a nonlinear constrained optimization problem that considers future states. Algorithms, such as GA, PSO, QP interior-point, and SQP, are used to solve the problem formulated.
5) A controller hardware-in-the-loop (CHIL) implementation of the proposed controller in a real-time simulation environment that demonstrates and validates its utility in a real-world scenario. Real-time CHIL tests have proven to be an effective tool for validating the performance of control systems under a more realistic scenario [26].

II. METHODOLOGY: ENERGY MANAGEMENT OF MICROGRIDS USING SBMPC

The proposed model, shown conceptually in Fig. 1, is a source allocation control scheme that considers various power sources (PV, energy storage, and grid) to meet the load requirements while minimizing the total cost of energy. One significant advantage that the proposed model has when compared with the other energy management models explored in the literature review is that the energy management solutions or setpoints gave by the controller consider both the current status of the system and its future (forecasted) states with considerably lower utilization of computing resources. This is achieved by formulating the energy management of the DERs as a shortest path problem, where the states of DERs are used to generate a graph that is searched, using a searching algorithm, with the objective of finding the ideal setpoints of all the DERs along the desired forecasting horizon. A detailed performance comparison between the different evaluated models is presented in Section IV.

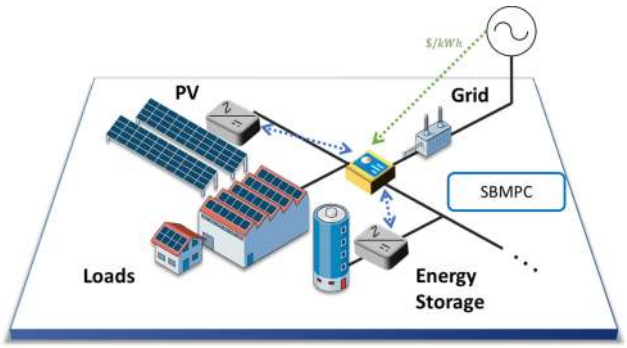

FIGURE 1. **Conceptual illustration of microgrid system with SBMPC controller.**

A. PROBLEM FORMULATION

The problem formulation is based on the energy management formulation of a microgrid similar to the one seen in Fig. 1, where the cost function is chosen to be the dollar cost of energy of the system over the entire forecasting horizon. The cost function to minimize is described as follows:

$$J(t_k) = [r_G(t_k)P_G(t_k) + s_{cd}(t_k)\, r_{ES} P^*_{ES}(t_k)]\Delta t \tag{1}$$

$$J_{total} = \sum_{k=0}^{N} J(t_{k+N}), \tag{2}$$

where $\Delta t = t_k - t_{k-1}$ (for all k) and

$$r_G(t_k) = \begin{cases} w\bar{r}_G(t_k), & \text{if } P_G(t_k) < 0, \\ \bar{r}_G(t_k), & \text{if } P_G(t_k) \geq 0 \end{cases} \tag{3}$$

Here, $J(t_{k+N})$ is the cost incurred from time $t_{k=0}$ to t_{k+N}, where N is the number of time steps along the forecasting horizon. P_G represents the power to or from the grid as seen at the point of common coupling (PCC) and is defined by (5). The value $P^*_{ES}(t_k)$ is the selected ES power setpoint, for charging/discharging operations, computed based on the result given by the EM controller. A negative $P_{ES}(t_k)$ value represents charging while a positive $P_{ES}(t_k)$ value represents discharging. r_G and r_{ES} represent the price rates (in \$/kWh) associated with the grid and ES, respectively. The weight, w, is chosen on the interval $0 < w < 1$ so as to incorporate differential pricing that distinguishes the sell-to-grid and buy-from-grid price rates. This helps the optimization algorithm to prioritize charging or discharging operations of the ES based on different buy-sell price scenarios. In (1), the value 0 for the binary variable $s_{cd}(t_k)$ represents the charging operation of the ES system, while the value 1 represents the discharging operation of the ES system.

$$s_{cd}(t_k) \in \{0, 1\} \tag{4}$$

The defined cost function must satisfy different problem constraints such as the power balance at the point of common coupling (PCC), and the ratings for all the DER systems. The power balance at the PCC of the system is given as:

$$P_G(t_k) = \sum_{l=1}^{N_L} P^l_L(t_k) - \sum_{j=1}^{N_g} P^j_{PV}(t_k) - P^*_{ES}(t_k), \tag{5}$$

where P_G is defined as the power as seen from the grid perspective, and P^l_L is the active power from the loads in N_L. P^j_{PV} represents the PV power from the j PV system in the microgrid and r^j_{PV} is the levelized cost of energy (LCOE) for the j PV system in the set of N_g PV systems. The solutions given by the EM controllers must satisfy constraints from the grid, PV systems, and the ES system. These constraints are shown below:

$$P^{j,\min}_{PV} \le P^j_{PV}(t_k) \le P^{j,\max}_{PV} \tag{6}$$
$$Q^{j,\min}_{PV} \le Q^j_{PV}(t_k) \le Q^{j,\max}_{PV} \tag{7}$$
$$(S^j_{PV})^2 \ge (P^j_{PV}(t_k))^2 + (Q^j_{PV}(t_k))^2 \tag{8}$$
$$P_G(t_k) \le P^{\max}_G \tag{9}$$
$$P^{\min}_{ES} \le P_{ES}(t_k) \le P^{\max}_{ES} \tag{10}$$
$$Q^{\min}_{ES} \le Q_{ES}(t_k) \le Q^{\max}_{ES} \tag{11}$$
$$(S^2_{ES}) \ge (P^2_{ES}(t_k)) + (Q^2_{ES}(t_k)) \tag{12}$$
$$SOC^{\min}_{ES} \le SOC_{ES}(t_k) \le SOC^{\max}_{ES} \tag{13}$$

The constraints guarantee that all the systems in the microgrid are operating under their limiting capacity. These constraints define the limits on the apparent power (S), active power (P), and reactive power (Q) of all the sources connected to the microgrid system. The limits on the state-of-charge (SOC) of the ES system are also defined above. The state-of-charge for the next time ($SOC_{ES}(t_{k+1})$) is defined as:

$$SOC_{ES}(t_{k+1}) = SOC_{ES}(t_k) - \Delta SOC(t_k) \tag{14}$$

where ΔSOC is the state-of-charge variation during the charge or discharge process. ΔSOC is defined as

$$\Delta SOC(t_k) = \begin{cases} \eta_c \dfrac{P^*_{ES}(t_k) \cdot \Delta t}{E^{max}_{ES}}, & \text{when charging.} \\ \eta_d \dfrac{P^*_{ES}(t_k) \cdot \Delta t}{E^{max}_{ES}}, & \text{when discharging.} \end{cases} \tag{15}$$

Here E^{max}_{ES} is the maximum rated energy of the ES system and η_c and η_d are the efficiencies for either the charging or discharging operation of the battery. Due to this definition, the optimization problem needs to be treated as a non-smooth nonlinear programming optimization problem. It should be noted how this function definition does not represent a problem for SBMPC since the solutions are based on sampling, but for the QP and SQP approaches, this definition needs to be simplified.

B. EXTENDED NONLINEAR CONSTRAINED OPTIMIZATION FORMULATION CONSIDERING FUTURE STATES - GA, PSO, QP(IP) AND SQP

The energy management (EM) problem formulated above can be solved considering only the current status of the system, i.e., just optimizing for the current time-step, or considering the current and future states of the system, i.e., optimizing for the entire forecasting horizon. Here, we explain how the formulation presented above can be extended to solve the EM problem considering the current and future states of the system using a nonlinear constrained optimization approach. This formulation can be used to solve the EM problem as a deterministic or stochastic problem given some predicted/forecasted states. Using this formulation, the problem becomes a constrained nonlinear optimization problem in which quadratic programming, genetic algorithms (GA), or particle swarm optimization (PSO) can be used as the primary optimization technique to find the 'optimal' control values.

In order to simplify the explanation and without loss of generality, let us assume the problem only requires to take into consideration one variable load and one PV system. Using this assumption, (5) can be simplified as:

$$P_G(t_k) = P_L(t_k) - P_{PV}(t_k) - P^*_{ES}(t_k) \tag{16}$$

Additionally, to simplify notation, let us define the following variables as:

$$\mathbf{s^k_{cd}} = [s^0_{cd}, s^1_{cd}, ..., s^N_{cd}] \tag{17}$$
$$\mathbf{P^k_{ES}} = [P^0_{ES}, P^1_{ES}, ..., P^N_{ES}] \tag{18}$$

Where $\mathbf{s_{cd}}$ is the vector that contains the binary variables $s_{cd}(t_k)$, from $k = 0$ to N, and $\mathbf{P_{ES}}$ is the vector containing

the values to minimize the scalar cost function J_{total} subject to some nonlinear constraints and bounds. Using this notation, the cost function to minimize can be expanded and rewritten as:

$$\begin{aligned} J_{total} &= \Big[[r_G(t_0)(P_L(t_0) - P_{PV}(t_0) - P^0_{ES}) + s^0_{cd}(r_{ES}\ P^0_{ES})] \\ &\quad + [r_G(t_1)(P_L(t_1) - P_{PV}(t_0) - P^1_{ES}) + s^1_{cd}(r_{ES}\ P^1_{ES})] \\ &\quad ... + [r_G(t_N)(P_L(t_N) - P_{PV}(t_N) - P^N_{ES}) + ... \\ &\quad ... s^N_{cd}(r_{ES}P^N_{ES})]\Big]\Delta t \\ &= \sum_{k=0}^{N}[r_G(t_k)P_G(t_k) + s^k_{cd}\ r_{ES}P^k_{ES}]\Delta t \end{aligned} \tag{19}$$

The upper (UB) and lower bounds (LB) of the control vector variable $\mathbf{P_{ES}}$ ($LB \leq \mathbf{P_{ES}} \leq UB$) are defined by (10). Finally, the nonlinear constraints of this problem are associated with the state-of-charge (SOC) of the controlled energy storage (ES) system propagated through the forecasting horizon. In essence, at any time t_k, the value of P^k_{ES} must be constrained by the change in SOC that it will cause. If this change causes the SOC to go below or above the SOC limits defined by the problem, then that specific value of P^k_{ES} is not considered as a feasible solution. In other words, at every time step, the following constraint must be enforced:

$$SOC^{\min}_{ES} \leq SOC^{prev}_{ES} - P^k_{ES}\ \eta^k_{cd}\ (\frac{\Delta t}{E^{max}_{ES}}) \leq SOC^{\max}_{ES} \tag{20}$$

Where E^{max}_{ES} is the maximum energy rating of the ES system, η^k_{cd} is the efficiency for either the charging or discharging operation of the energy storage (ES) system, and SOC^{prev}_{ES} is the state-of-charge (SOC) of the ES system before the control action at t_k. As seen in this term, the value $(\frac{\Delta t}{E^{max}_{ES}})$ can be defined as a constant value since both E^{max}_{ES} and Δt are constant throughout the optimization procedure. The constant letter ζ will be used to define this value as seen in:

$$\zeta = (\frac{\Delta t}{E^{max}_{ES}}) \tag{21}$$

Using these definitions, we can characterize all the nonlinear constraints of the problem needed to perform the minimization of the cost function, while taking into account all the states starting from the current state $k = 0$ up to the end of the forecasting horizon at $k = N$. These constraints are presented in (23)-(28), shown at the bottom of this page. Note that these nonlinear constraints are defined using the standard form $c(x) \leq 0$.

C. SAMPLING-BASED MODEL PREDICTIVE CONTROL ENERGY MANAGEMENT SOLUTION

Sampling-Based Model Predictive Control (SBMPC) is an MPC method that consists of the consolidation of an optimization algorithm called Sampling-Based Model Predictive Optimization (SBMPO) and a receding horizon control technique [27], [28]. The main idea behind using SBMPC to solve the energy management problem, formulated in the previous section, relies on the concept that this problem can be formulated as a shortest path problem. In this shortest path problem, the nodes of the graph represent the different states of the system, and the edges represent the cost associated with moving to a particular state at each time step t_k. In essence, SBMPC creates a graph tree that is searched using a searching algorithm designed to find the optimal path of actions from the current state of the system up to the system state at the end of the prediction horizon. In our particular case, the A* search algorithm is the algorithm used to traverse the graph. The pseudocode listing of the SBMPC algorithm is presented in Algorithm 1. The main details of this algorithm are explained below.

SBMPC performs an iterative search that searches through a graph that is generated based on forecasted microgrid system states and a propagation model of the energy storage being controlled by SBMPC. This iterative process starts from the current state at $t_k = 0$ and runs up to the prediction horizon, t_N. At each time step (from k to N), the current node with the lowest cost is expanded into a diverse pool of possible states that the microgrid system can end up based on the forecasted values and the control setpoint of the ES system. After these states are expanded, they are checked against constraints and prune based on similarity criteria before they are added to the final graph tree. This process is done to reduce the size of the graph that is going to be searched. Finally, the nodes that are added to the final graph are evaluated based on their individual cost, and a path that connects the nodes with the lowest costs is obtained as a result. Fig. 2 presents an overall depiction of the solution

$$P^0_{ES}\ (\eta^0_{cd} \times \zeta)\ - SOC^{\text{init}}_{ES} + SOC^{\min}_{ES} \leq 0 \tag{23}$$
$$-P^0_{ES}\ (\eta^0_{cd} \times \zeta) + SOC^{\text{init}}_{ES} - SOC^{\max}_{ES} \leq 0 \tag{24}$$
$$P^1_{ES}\ (\eta^1_{cd} \times \zeta)\ - (SOC^{\text{init}}_{ES} - P^0_{ES}\ (\eta^0_{cd} \times \zeta)) + SOC^{\min}_{ES} \leq 0 \tag{25}$$
$$-P^1_{ES}\ (\eta^1_{cd} \times \zeta) + (SOC^{\text{init}}_{ES} - P^0_{ES}\ (\eta^0_{cd} \times \zeta)) - SOC^{\max}_{ES} \leq 0 \tag{26}$$
$$\dots$$
$$P^N_{ES}(\eta^N_{cd} \times \zeta)\ -(SOC^{\text{init}}_{ES} - P^0_{ES}\ (\eta^0_{cd} \times \zeta) - P^1_{ES}\ (\eta^1_{cd} \times \zeta)... - P^{N-1}_{ES}\ (\eta^{N-1}_{cd} \times \zeta)) + SOC^{\min}_{ES} \leq 0 \tag{27}$$
$$-P^N_{ES}(\eta^N_{cd} \times \zeta)\ +(SOC^{\text{init}}_{ES} - P^0_{ES}\ (\eta^0_{cd} \times \zeta) - P^1_{ES}\ (\eta^1_{cd} \times \zeta)... - P^{N-1}_{ES}\ (\eta^{N-1}_{cd} \times \zeta)) - SOC^{\max}_{ES} \leq 0 \tag{28}$$

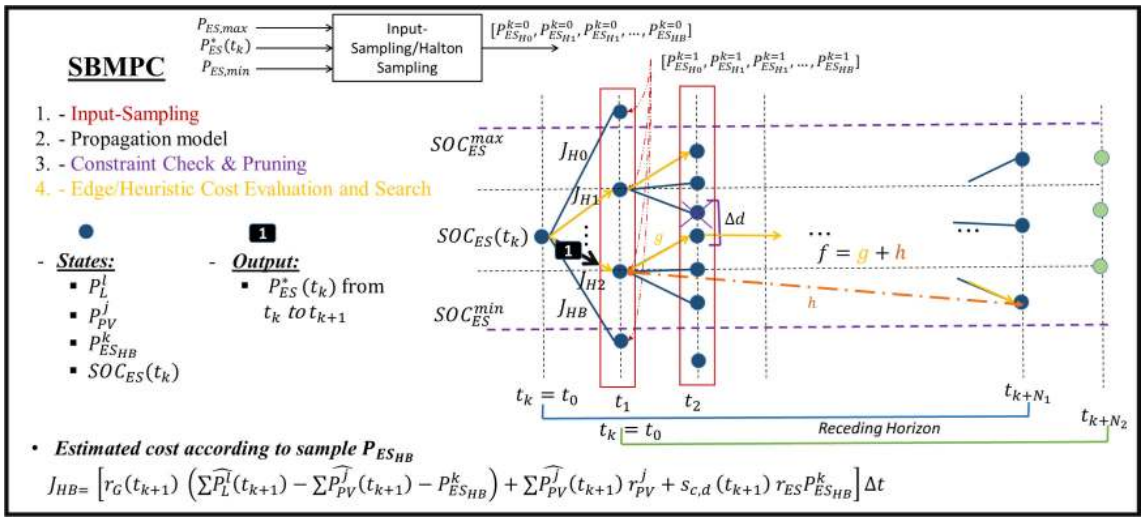

FIGURE 2. **Sampling-Based Model Predictive Control (SBMPC) for energy management of microgrid system. This diagram shows the 4 major steps executed by the SBMPC algorithm and their relationships. SBMPC is executed continuously with a receding horizon, so at every new step SBMPC is re-executed.**

Algorithm 1 SBMPC Algorithm

Input: *system_states*(t_k)
Output: *control_action*(t_k)
Initialisation : time-step (k), branchout factor (B), predict. horizon (N) Open_List ← *start_node*, Closed_List ← 0

while (*stopping_criteria*) **do**
  for $k = 0$ to N **do**
    Select node w/ highest priority in Open List;
    Move expanded node into Closed List;
    for $j = 0$ to B **do**
      Sample control space;
      Propagate system model;
      Determine *neigh_nodes* of current node;
      if (*neigh_nodes* **don't satisfy** constraints) **then**
        Remove *neigh_nodes* from list;
      else
        Add *neigh_nodes* to graph (Open_List);
      end if
      Evaluate node cost based on cost (g) and heuristic (h): $f(k) = g + h$;
    end for
  end for
  Construct *optimal_trajectory*;
end while
Get *control_action*(t_k) from *optimal_trajectory* ;
return *control_action*(t_k)

process performed by SBMPC and shows how SBMPC is able to reformulate the energy management problem as a shortest path problem that is solved finding the optimal path through the generated graph. The major steps that are executed by SBMPC during the iterative search procedure are:

1) Input-Sampling of controlled model
2) Propagation/Forecasting model for system states
3) Constraints checks and pruning
4) Edge/Heuristic cost evaluation and A* search procedure

1) INPUT-SAMPLING

At each control time step t_k, SBMPC implements an input-sampling procedure by discretizing the continuous state space of the controlled model into a feasible region of inputs. In our case, Halton sampling is used to sample the possible states of the ES system. This deterministic sampling procedure is necessary due to the fact that the possible states of the ES system lie in a continuous space; thus, discretization is needed for the proposed discrete control. Halton sampling is used due to its advantage of limiting dimensionality and low discrepancy when compared to other sampling methods such as random sampling and gridding [29]. Fig. 3 shows how the Halton sampling procedure is performed and the differences between pseudorandom, gridding, and Halton on the sampled space. The sample values of the ES system are generated based on the current or estimated states of the node being expanded and are propagated (using the propagation models) until the end of the forecasting horizon. The number of samples generated by the input-sampling procedure is limited by a factor called the *branchout factor*, (B), that will determine the number of branches of the tree that emanate from a particular node based on the sampled values.

2) PROPAGATION MODEL

SBMPC is an algorithm that computes a graph tree with nodes and branches generated from samples given by the input-sampling procedure and a propagation model. As described in [28], the propagation model can be modeled

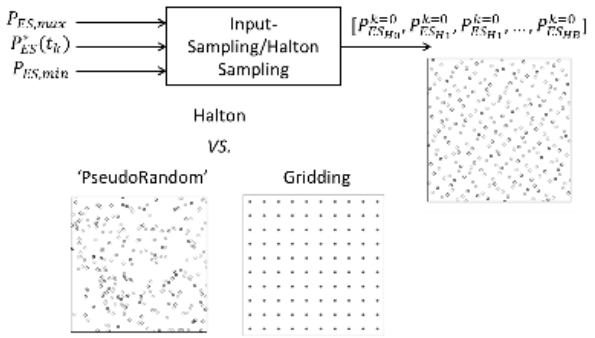

FIGURE 3. SBMPC input-sampling procedure using Halton sampling. Halton sampling vs. Pseudorandom sampling vs. Gridding. Others sampling models can be used, but SBMPC relies primarily on Halton sampling.

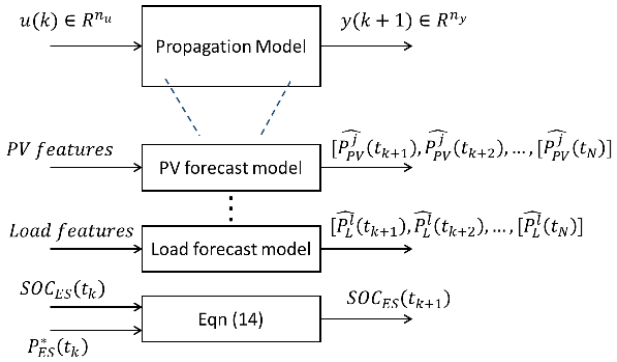

FIGURE 4. SBMPC propagation model. SBMPC needs the forecast of the future states of the microgrid system (PV power generation, load consumption, SOC_{ES}).

as a nonlinear discrete-time model or using machine learning models such as neural networks. In our case, the propagation model is in charge of producing a forecast or estimation of the future system states. Particularly, (14) is used as the propagation model for the state of charge of the ES system (SOC_{ES}) while the forecast of the PV power generation and the cumulative load consumption, until the end of the forecasting horizon (24 hours in 15 minutes steps), is propagated based on machine learning models. It is important to note that SBMPC is not restricted to any particular forecasting model. The training, validation, and testing results for the forecasting models are presented in Section III. Fig. 4 shows a general depiction of the propagation models.

3) CONSTRAINTS CHECK AND PRUNING

After the states of the system (nodes to add to the graph) are obtained from the sampling procedure and the propagation models, the node at t_k is expanded into a diverse pool of possible states at t_{k+1} that are represented by the new 'neighbor' nodes that are going to be added to the graph and connected to the current node being explored. As mentioned previously, the expansion of the current node is limited by the branchout factor. Before these nodes are added to the graph, all the new 'neighbor' nodes, which represent different states of the microgrid system, are checked against all the constraints defined by (6)-(13). In other words, all these new possible states of the system are checked against all the constraints defined, and the nodes that do not comply with these constraints are dropped from the final graph.

In addition to the constraints check procedure, a pruning mechanism was introduced in order to reduce redundancy in the generation of new 'neighbor' nodes. The pruning mechanism consists in the elimination of all the nodes/branches that exist in the same time step (t_{k+n}) and have a small enough Δd difference in cost and value with a node that already exists in the graph. This procedure improves the searching time considerably, i.e., the execution time of SBMPC, because it prevents the creation of branches that are equivalent to already existing branches.

4) EDGE/HEURISTIC COST EVALUATION AND A* SEARCH PROCEDURE

After the previous steps are executed, the new 'neighbor' nodes are connected to the current expanded node, and their edge and heuristic costs are generated according to the cost function of the problem being optimized. The edge cost is defined as the cost to move from node to node, and the heuristic cost is defined as the *optimistic* (lower bound) to move from the current node to the goal. As seen in Fig. 2, the edge cost (g) is calculated as J_{HB}, where B represents a number between 1 and the total number of branches generated during the Halton sampling procedure. Similarly, the heuristic cost (h) is defined as the optimistic estimation that the predicted load at any time step can be fulfilled entirely by the cheapest power source for that time interval. In other words, it is represented by the summation of the lowest cost terms associated with each power source. Fig. 5 shows the description of the heuristic used. In any instance, this formulation meets the necessary condition for optimality needed in the A* search algorithm (i.e., a rigorous lower bound on the cost-to-goal) [30]. (22) shows the total cost for moving from node to the other, taking into account the heuristic cost.

$$f = g + h \tag{22}$$

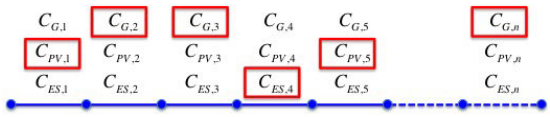

$$C_{G,k} = r_G(t_k)P_G(t_k)\Delta t$$
$$C_{PV,k} = r_{PV}P_{PV}(t_k)\Delta t$$
$$C_{ES,k} = r_{ES}P_{ES}(t_k)\Delta t$$

$$H = C_{PV,1} + C_{G,2} + C_{G,3} + C_{ES,4} + C_{PV,5} + \cdots + C_{PV,n}$$

FIGURE 5. Heuristic used for Sampling-Based Model Predictive Optimization. The lowest cost terms are highlighted in (red) boxes on the time line.

While the graph is being iteratively generated, SBMPC searches the tree using the well-known A* algorithm [30]. SBMPC uses the A* search algorithm as its main searching procedure in order to find the lowest 'cost' path of actions/system states from the current time step, $t_{k=0}$, up to the forecasting horizon at $t_{k=N}$ (in our particular case, 24 hours later or $N = 96$). This 'optimal' trajectory is constructed at the same time the search is being executed since each node visited while searching the graph is stored in priority queue with information regarding its overall f cost and its parent nodes. Finally, after the 'optimal' trajectory is extracted, the current ideal control action at $t_k = 0$ is extracted from the defined trajectory and applied to the controlled system.

III. EXPERIMENTAL SETUP

To test the proposed control scheme, distribution network data, solar generation profiles, and load profiles were obtained from different available open-source databases. The data obtained was formatted and pre-processed for modeling the distribution network simulation and the development of the forecasting models.

A. PROPAGATION MODEL: TRAINING, VALIDATION, AND TESTING OF NEURAL NETWORKS

The forecasting model used to perform the PV power forecasting of the system consists of a modified version of the forecasting model presented in [31]. The neural network model for forecasting the load demand consists of a feed-forward DNN with 9 input parameters, 2 hidden layers with 5 neurons in each layer, and 1 output neuron representing the forecasted load power demand at the specific time. The input parameters are: the hour of the day (0-23), the minutes of the hour (0, 15, 30, 45), the month number (1-12), day of the week (1-7), is weekend (0-1), forecasted temperature, season: winter, spring, summer, fall (1-4), load value 24 hours before, and the load value 168 hours before (1 week before).

1) SOLAR DATA (SUNGRIN AND NREL)

The solar data used to develop the solar PV forecasting model (training, validation, and testing) was obtained from the SUNGRIN report [32]. This report has solar PV generation data from different large-scale solar PV systems around the state of Florida. Additional temperature data were obtained from the National Solar Radiation Database (NSRDB) from NREL. The forecasting model was trained, validated, and tested using 70,176 samples of 15-minute interval data. The data was split into a training set (70%), validation set (15%), and testing set (15%). The metrics used for evaluating the performance and accuracy of this forecasting model were: the root mean squared error (RMSE), the normalized root mean squared error (NRMSE), the coefficient of determination (R), and the mean absolute percentage error (MAPE) as defined by NREL in [33]. Table 1 presents the result metrics selected for evaluating the performance and accuracy of the forecasting model.

2) LOAD DATA (SUNGRIN AND CITY OF TALLAHASSEE)

The load data and load profiles used were also obtained from the SUNGRIN project database, which has network model data and aggregated load profiles from various feeders located around the state of Florida [32]. Additional information was obtained from the City of Tallahassee energy consumption database. The neural network model was trained, validated, and tested using 35,200 samples of 15-minute interval data. The data was split into a training set (70%), validation set (15%), and testing set (15%). The same metrics were used for evaluating the performance and accuracy of this forecasting model. Table 1 presents the result metrics selected for assessing the performance and accuracy of the model.

TABLE 1. PV and Load forecasting results performance.

Forecasting Metrics	PV	Load
RMSE (kW)	70.67	24.12
NRMSE	0.095	0.052
MAPE (%)	4.96	3.52
R	0.97	0.95

B. SIZING OF THE TEST CASE AND MODEL

For testing the proposed controller, the load, PV system, and energy storage systems were sized according to a large-scale commercial/ industrial or campus scale micro-grid application. The load profile used for this study is modeled as a 15-minute resolution variable load with a maximum of 850 kW, a minimum of 406 kW, and an average of 544 kW over 7-days simulated. Particularly, 7-days of simulation were chosen so all control tests can be evaluated under different types of scenarios continuously (e.g., sunny days, rainy days, high RTP prices, etc.), and to have a reasonable simulation time for the real-time simulation. The rating of the PV system and the energy storage system are presented in Table 2. The energy storage system was modeled according to currently available utility-scale solutions with a maximum capacity of 2190 kWh.

TABLE 2. PV and Energy Storage (ES) system specifications.

System Parameters	ES	PV
ES Rating ($P_{ES/PV}$)	750 kW	875 kW
Inverter Rating ($S_{ES/PV}$)	750 kVA	900 kVA
Max. Energy at 100% SOC ($SOC_{ES}^{\max}$)	2190 kWh	NA
Min. Energy at 10% SOC ($SOC_{ES}^{\min}$)	219 kWh	NA
Power Factor Range ($pf_{ES/PV}$)	0.8-1.0	0.8-1.0
Max. Reactive Power ($Q_{ES/PV}^{\max}$)	450 kVAR	540 kVAR
Min. Reactive Power ($Q_{ES/PV}^{\min}$)	-450 kVAR	-540 kVAR
LCOE ($r_{ES/PV}$)	12.3 c/kWh	2.51 c/kWh

C. REAL-TIME PRICE AND LEVELIZED COST OF ENERGY FOR ES AND PV SYSTEMS - r_G, r_{PV}, AND r_{ES}

The real-time price (r_G) data was obtained by adjusting the publicly available New York Independent Service

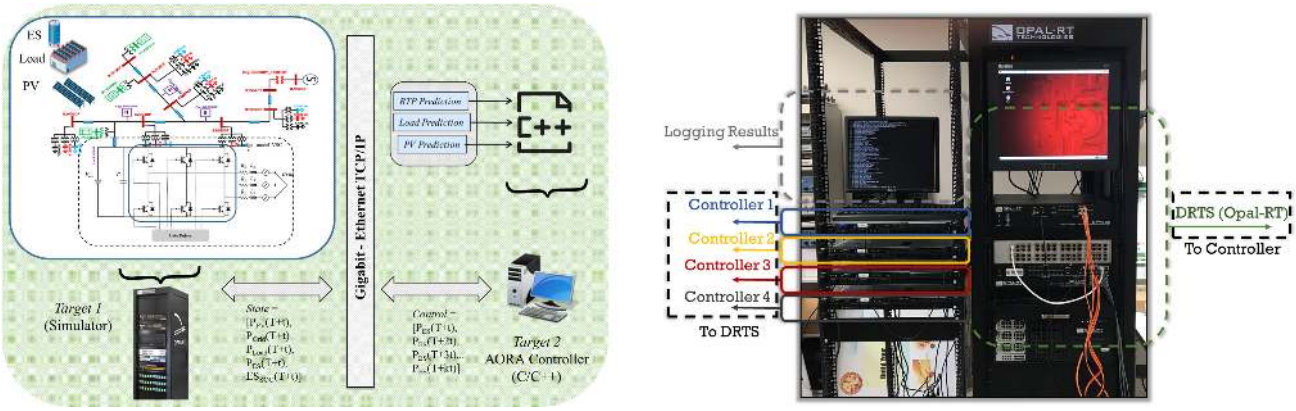

(a) Block layout of hardware setup for the CHIL simulation

(b) CHIL Implementation: Controllers and DRTS

FIGURE 6. (a) Block diagram of controller Hardware-in-the-loop (CHIL) Communication, and (b) Implementation setup.

Operator (NYISO) wholesale location-based marginal pricing (LBMP) as a real-time price (RTP) and using City of Tallahassee time-of-use (ToU) based retail rates. The modification of the price consists of the addition of an RTP supplier charge plus the addition of an off-peak or on-peak rate (bias) appropriate to North Florida load patterns and markets. For the PV system, the levelized cost of energy (LCOE) of the system was calculated with the objective of generating an estimated cost of using the PV system. Similarly, since SBMPC requires knowledge of the cost of using the energy storage system, a similar approach to [34] was used to calculate a price rate r_{ES} for the energy storage (ES) system. The equation used was:

$$r_{ES} = \frac{C_{total}^{ES}}{Cyc \cdot E_{ES}^{max} \cdot DoD \cdot \eta_r}, \tag{23}$$

where C_{total}^{ES} is the total cost of the ES system, DoD is the desired depth-of-discharge of the ES system, Cyc is the total number of cycles under warranty at depth-of-discharge, E_{ES}^{max} is the total energy capacity of the ES system, and η_r is the round-trip efficiency of the system.

D. OFFLINE AND CONTROLLER HARDWARE-IN-THE-LOOP (CHIL) SIMULATION

An average-value based inverter model of a three-phase two-level voltage-source converter (VSC) is used to validate the performance of the SBMPC controller in both offline and controller hardware-in-the-loop implementations. These VSCs are connected to the PV and ES system. The energy storage model used for simulating the behavior of the Li-Ion battery used was taken from MATLAB/Simulink. This model is based on the charge and discharge models presented in [35]. The load model used for the system is based on a dynamic load profile in which the active and the reactive power of the load changes dynamically every 15 minutes along the span of the simulation.

1) OFFLINE SIMULATION

An offline simulation of the system and the SBMPC controller is performed using phasor models of the PV system, dynamic load, ES, and feeder. The SBMPC controller is developed in C/C++. The objective of this simulation is to ensure the proper control and execution of the controller while performing simulations for extended periods of time (1 to 7 days). The results of the offline simulation are verified using MATLAB/Simulink software, and the cost is calculated according to the cost function presented.

2) CONTROLLER HARDWARE-IN-THE-LOOP (CHIL) SIMULATION

A controller hardware-in-the-loop (CHIL) system is comprised of a physical hardware controller that interacts with a simulated software system in a real-time environment. In this case, the entire electrical/power system (PV system, ES, load, and grid) is modeled inside the simulator. All the components inside the power system are modeled with a 50-μs simulation time step. The C/C++ code of the SBMPC controller is installed and executed on external physical hardware with a CPU clock speed of 3.4 GHz, 8 GB of RAM and running a Linux distribution. Simulink, SimPowerSystems, and RT-LAB are the main programs used for developing, loading, and running the models for the CHIL simulation. As seen in Fig. 6, the real-time power system models are loaded on *Target 1*, and the SBMPC controller code is loaded on *Target 2*. The communication between the two targets is performed using TCP/IP protocol and a network switch that facilitates the connection between them. As observed in Fig. 6a, the simulator (*Target 1*), simulates the electrical system and sends the current state of the system (PV generation, load consumption, grid consumption, ES charging/discharging and ES state of charge (SOC)) to the SBMPC controller through the TCP/IP connection. After receiving the states, the controller produces the required predictions, performs the sampled-based model predictive

optimization (SBMPC) operation, and sends the control signals to the ES system inside the real-time simulator. Currently, for a 24-hour planning trajectory, the model takes about 1.5 to 2.0 seconds to execute the optimization algorithm and send the decision trajectory back to the simulated power system on *Target 1*.

IV. EXPERIMENTAL RESULTS

For a thorough comparison, the performance of the SBMPC controller is evaluated against other baseline cases such as two manual control cases and four optimization algorithms (genetic algorithm (GA), particle swarm optimization (PSO), QP interior-point method (QP-IP), and sequential quadratic programming (SQP)). In the two manual control cases, the charge and discharge operations are performed based on preset control actions. Case 1 charges the ES between 2 am and 5 am and discharges it between 7 pm and 11 pm. Case 2 performs the charge operation for the ES between 11 am and 2 pm, and discharges the ES at the same time as Case 1 (7 pm to 11 pm). Case 1 exemplifies a case where users preset the charge of the ES at the presumed lower price period while Case 2 shows how a user presets the charge of the ES at times when the PV system is presumed to have maximum power output. Both cases discharge at the presumed higher price period of the RTP signal. In the case of GA, PSO, QP(IP), and SQP, two cases for each model are evaluated: a) optimization considering only the current status of the system (i.e., no forecast), and b) optimization considering current and future states of the system (i.e., formulation presented in Section II-B). All the models are evaluated according to their achieved cost at the end of the simulation and their average computation time for execution. It is important to note that all the models that consider the future states of the system use the same forecast profiles generated by the forecasting module. Both offline and CHIL implementations are simulated for 7-days using the data described in the previous sections.

A. OFFLINE SIMULATION RESULTS

For the offline implementation, three ES price scenarios are used for comparing and testing the performance of the SBMPC controller (SBMPC) against Case 1 and 2, GA^a, PSO^a, $QP(IP)^a$, SQP^a, GA^b, PSO^b, $QP(IP)^b$, and SQP^b. The superscripts *a* and *b* are used to distinguish between the two cases previously explained. The three ES prices used for testing the performance of the models are: $r_{ES} =$ 12.3, 7.0, 5.3 c/kWh. These prices were calculated according to the cost of currently available energy storage systems of the size proposed. Each test case is run for 7 days, and costs are calculated for the entire system during the span of the simulation. The SOC of the energy storage at the beginning of the simulation is at the minimum 10%. This ensures that the test cases and algorithms are starting with no "free charge" and must find the best charge and discharge control actions in order to minimize the overall cost.

TABLE 3. Cost comparison results for offline tests.

Control Technique	r_{ES} (c/kWh)			*Execution Time (s)*
	12.3	**7.0**	**5.3**	
Case 1	$ 6,187.50	$ 5,538.10	$ 5,329.80	-
Case 2	$ 6,811.20	$ 6,161.70	$ 5,953.40	-
GA^a	$ 5,155.00	$ 5,190.60	$ 5,144.20	4.26
PSO^a	$ 5,155.00	$ 5,190.60	$ 5,144.20	6.54
$QP(IP)^a$	$ 5,155.00	$ 5,190.60	$ 5,144.20	0.04
SQP^a	$ 5,155.00	$ 5,190.60	$ 5,144.20	0.132
GA^b	$ 4,876.21	$ 4,742.38	$ 4,645.50	128.35
PSO^b	$ 6,047.40	$ 5,585.90	$ 5,226.01	275.66
$QP(IP)^b$	$ 4,954.45	$ 4,748.80	$ 4,683.93	1.31
SQP^b	$ 4,842.24	$ 4,671.77	$ 4,576.76	4.43
SBMPC	$ **4,842.70**	$ **4,702.30**	$ **4,609.30**	**1.96**
% savings wrt Case 1	21.70 %	15.10 %	13.50 %	-
% savings wrt Case 2	28.90 %	23.70 %	22.6 %	-
% savings wrt GA^a	6.06 %	9.41 %	10.40 %	2.2x faster
% savings wrt PSO^a	6.06 %	9.41 %	10.40 %	3.3x faster
% savings wrt $QP(IP)^a$	6.06 %	9.41 %	10.40 %	49.0x slower
% savings wrt SQP^a	6.06 %	9.41 %	10.40 %	14.8x slower
% savings wrt GA^b	0.69 %	0.85 %	0.78 %	65.4x faster
% savings wrt PSO^b	19.9 %	15.82 %	11.80 %	140.6x faster
% savings wrt $QP(IP)^b$	2.31 %	1.00 %	1.62 %	1.50x slower
% savings wrt SQP^b	-0.01 %	-0.65 %	-0.71 %	2.2x faster

Table 3 presents the results with cost comparisons between all the evaluated cases. As observed, the SBMPC controller is able to provide savings from 6.06% up to 28.9% when compared with the manual cases and the optimization cases that only take into account the current state of the system. All these baselines test algorithms (GA^a, PSO^a, $QP(IP)^a$, and SQP^a) are able to achieve the same cost along the span of the simulation, but when compared with the SBMPC approach, they demonstrate a clear disadvantage due to optimizers considering only the current status of the system. Note also that all four baseline algorithms (GA^a, PSO^a, $QP(IP)^a$, and SQP^a) achieved a lower cost when the price of ES is at the highest price ($r_{ES} = 12.3$ c/kWh) due to the fact that it's only economically feasible to discharge at highest price peaks, so they are forced to wait until these peaks occur in order to dispatch. In contrast, SBMPC (together with GA^b, PSO^b, SQP^b, and SQP^b) are not affected because they are able to plan and delay immediate rewards (lower costs), at all ES prices, to perform charging actions at the lowest periods and discharging operations at the highest periods along the forecasting horizon. This is one of the primary advantages demonstrated by the model presented in this paper.

On the other hand, Table 3 clearly demonstrates how SBMPC is able to achieve a slightly better cost when compared to GA^b with a significant reduction in execution time for the entire forecasting horizon (96 steps). When compared with $QP(IP)^b$, SBMPC manages to achieve a better cost at all prices but has a slightly higher average execution time of around 0.65 seconds more. Additionally, when compared with the SQP^b model, SBMPC achieves a slightly worse cost between -0.01 % and -0.71 % in all cases tested but improves the execution time of the optimization process significantly. Note how PSO^b had terrible performance when used to solve the energy management problem considering

TABLE 4. Parameters used in models tested.

Model	Parameter Name	Value
SBMPC	Branchout factor (B)	17
	Prune difference (Δd)	0.01
	Sampling	Halton
GA[a,b]	Population Size	200
	Max. Generations	100
	Max. Stall Generations	20
	Initial Population	Uniform RNG
	Optimal Tolerance	1.0e-6
PSO[a,b]	Population Size	100[a], 600[b]
	Inertia weight max-min	0.9-0.4[a], 0.5-0.1[b]
	Acceleration factor 1, 2	2-2
	Max. Iterations	1000[a], 100[b]
	Optimal Tolerance	1.0e-6
QP(IP)[a,b]	Max. Iterations	3000[a], 9800[b]
	Solver	quadprog (interior-point)
	Optimal Tolerance	1.0e-8
SQP[a,b]	Max. Iterations	1000[a], 9800[b]
	Solver	fmincon
	Optimal Tolerance	1.0e-6

future states due to the high number of control variables it needed to optimize. Table 4 shows the parameters for all the models used in these test cases. These results exhibit some of the key advantages of formulating the energy management problem using a shortest path graph-search approach. These key advantages are related to the way the input state space is discretized and sampled from a continuous state space using an input-sampling procedure, and the way the problem is solved using a fast graph-searching algorithm. In other words, if the number of input control variables increase, e.g., adding more DER systems to control or extending the forecasting horizon, models such as SQP, GA, and PSO will significantly increase their computational time and computing resources, while a regular QP(IP) approach would yield a higher cost. In contrast, SBMPC has the ability to easily limit the dimensionality of the problem via the input-sampling procedure while sacrificing small deviations in the cost.

To further demonstrate this advantage, an additional energy storage (ES) system was introduced in the EM problem formulated above. The number of control variables for this case increase from 96 to 192. For this case, only the QP(IP), SQP, and SBMPC results are shown since the GA and PSO results yield non-competitive execution times and very high overall costs. Additionally, it is worth noting that for this case each ES system had different r_{ES}, where $r_{ES1} =$ 12.3 c/kWh and $r_{ES2} = 7.0$ c/kWh. In these tests, SBMPC yielded an overall cost of \$4,855.90 and an average execution time of 4.80 seconds. The QP(IP) method yielded an overall cost of \$4,882.90 and an average execution time of 2.01 seconds. Finally, SQP yielded the minimum overall cost with \$4,682.30 but the highest average execution time of around 11.02 seconds. Table 5 summarizes these results. These results demonstrate how SBMPC could be considered as a viable competitor to the studied approaches when solving nonlinear constrained optimization since it has the ability to achieve cost-effective solutions while keeping a low computational execution time.

TABLE 5. Cost and execution time comparison of PV-integrated system with 2 energy storages test cases.

Control technique	*Cost (\$)*	*Execution Time (s)*
QP(IP)[b]	4,882.90	2.01
SQP[b]	4,682.30	11.02
SBMPC	4,855.90	4.80

Based on the tests conducted, SBMPC was the third-fastest algorithm according to the average execution time at each time step for all the test cases, and the second-fastest when compared to the models optimizing based on forecasting profiles (with and without multiple ES systems). So, as demonstrated by these results, the use of SBMPC shows potential energy cost reductions in energy management problems with a low computational time demand when compared with current manual ES controls and optimization algorithms operating under variable energy price profiles.

B. CHIL SIMULATION RESULTS

For the CHIL (controller hardware-in-the-loop) implementation, 4 identical servers are used in parallel to run different ES price scenarios for the proposed SBMPC algorithm. The primary objective of this test is to demonstrate how the proposed SBMPC controller can be deployed in a real-world microgrid environment. Similarly to the offline tests, three ES prices used for testing the performance of the model: $r_{ES} =$ 12.3, 7.0, 5.3 c/kWh. The controllers are connected to the microgrid modeled in the real-time environment inside the digital real-time simulator (DRTS) (OPAL-RT) using a TCP/IP protocol interface, as explained earlier. Fig. 6b depicts the hardware CHIL setup.

The SBMPC costs for the 7-days real-time simulation for each r_{ES} price (12.3, 7.0, 5.3 c/kWh) were \$4,874.40 \$4,722.60, and \$4,628.60 respectively. The differences between the offline results and CHIL results (around 0.5% on average) can be accounted to the different characteristics presented by the models of the ES, load, and PV systems. As explained in Section III, the CHIL simulation includes more detailed models for each of the components and display more realistic results due to its real-time simulation in the transient domain, different from the offline model where the microgrid components are modeled in phasor domain. Fig. 7 show the SBMPC control actions performed in the 4th day of the 7-days CHIL simulation for the case $r_{ES} = 7.0$ c/kWh. As observed in the figure, the SBMPC controller controls the discharging operation of the ES only when the estimated cost of using the amount of power selected is lower than the cost of using the utility grid. It can also be observed that the charging operations are performed at some steps in anticipation of higher prices where the ES is used to offset the use of the grid at those high price times. Overall, results demonstrate the great potential of the proposed model for energy scheduling and energy management operations that

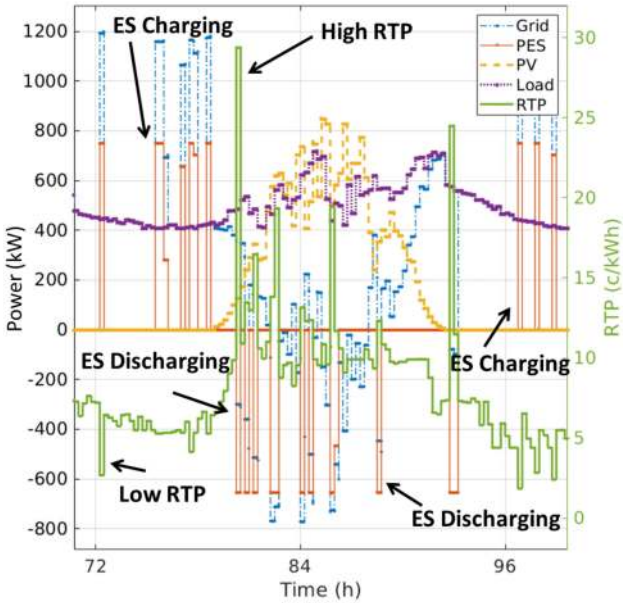

FIGURE 7. Power profile for 4th day of real-time CHIL simulation at 7.0 c/kWh ES price with SBMPC control.

rely on varying energy price schemes. Note that since the EM problem formulated minimizes the total cost of the localized energy consumption, the model 'solutions' can be obtained via finding the optimal mix of generating resources. This approach works under scenarios where all available DERs have different energy prices, and the grid provides an external energy price that is defined by the energy provider. Nonetheless, without the grid, e.g., off-grid microgrid, the proposed approach is capable of optimizing the available DERs based on their individual energy prices.

V. CONCLUSION

This paper proposed a novel energy management solution aimed to determine the cost-effective resource allocation of multiple DERs, such as PV and ES, in a large-scale site. The control scheme is designed to solve the energy management problem by using Sampling-Based Model Predictive Control (SBMPC) and converting the problem to a graph search approach. The proposed model is tested using realistic data from a feeder located in the state of Florida, together with reliable DER and load models developed for offline and real-time controller hardware-in-the-loop (CHIL) tests. Additionally, a detailed extended formulation for solving the nonlinear constrained optimization energy management problem is presented and used to compare the performance of other optimization techniques currently being used in the literature such as GA, PSO, QP(IP), and SQP. The results show performance improvement in the cost and execution time of the proposed SBMPC controller over the ten baseline test cases evaluated for their respective cases in a 7-day simulation span. Results demonstrate the controller's ability to respond to varying energy price schemes by optimizing the use of all the resources connected to the system to achieve a lower utilization cost. The employment of the proposed controller has the potential of providing incentives for the development of real-time price schemes that can be tailored for the use of optimal controllers aimed to reduce energy costs by operating at optimal times. Future work will focus on extending SBMPC to solve EM problems for distributions systems that include additional constraints, thermal-based DG systems, and other types of renewable DERs.

REFERENCES

[1] P. Denholm, K. Clark, and M. O'Connell, "On the path to sunshot—Emerging issues and challenges in integrating high levels of solar into the electrical generation and transmission system," Nat. Renew. Energy Lab., Golden, CO, USA, Tech. Rep. NREL/TP-6A20-658007617, 2016.

[2] J. Fedjaev, S. A. Amamra, and B. Francois, "Linear programming based optimization tool for day ahead energy management of a lithium-ion battery for an industrial microgrid," in *Proc. IEEE Int. Power Electron. Motion Control Conf. (PEMC)*, Sep. 2016, pp. 406–411.

[3] S. Lilla *et al.*, "Mixed integer programming model for the operation of an experimental low-voltage network," in *Proc. IEEE Manchester PowerTech*, Jun. 2017, pp. 1–6.

[4] Z. Chen, L. Wu, and Y. Fu, "Real-time price-based demand response management for residential appliances via stochastic optimization and robust optimization," *IEEE Trans. Smart Grid*, vol. 3, no. 4, pp. 1822–1831, Dec. 2012.

[5] P. Kou, D. Liang, and L. Gao, "Stochastic energy scheduling in microgrids considering the uncertainties in both supply and demand," *IEEE Syst. J.*, vol. 12, no. 3, pp. 2589–2600, Sep. 2018.

[6] M. S. Taha, H. H. Abdeltawab, and Y. A.-I. Mohamed, "An online energy management system for a grid-connected hybrid energy source," *IEEE J. Emerg. Sel. Topics Power Electron.*, vol. 6, no. 4, pp. 2015–2030, Dec. 2018.

[7] A. C. Luna, L. Meng, N. L. Diaz, M. Graells, J. C. Vasquez, and J. M. Guerrero, "Online energy management systems for microgrids: Experimental validation and assessment framework," *IEEE Trans. Power Electron.*, vol. 33, no. 3, pp. 2201–2215, Mar. 2018.

[8] W. Hu, P. Wang, and H. B. Gooi, "Toward optimal energy management of microgrids via robust two-stage optimization," *IEEE Trans. Smart Grid*, vol. 9, no. 2, pp. 1161–1174, Mar. 2018.

[9] C. Ju, P. Wang, L. Goel, and Y. Xu, "A two-layer energy management system for microgrids with hybrid energy storage considering degradation costs," *IEEE Trans. Smart Grid*, vol. 9, no. 6, pp. 6047–6057, Nov. 2018.

[10] H. Li, C. Zang, P. Zeng, H. Yu, and Z. Li, "A genetic algorithm-based hybrid optimization approach for microgrid energy management," in *Proc. IEEE Int. Conf. Cyber Technol. Automat., Control, Intell. Syst. (CYBER)*, Jun. 2015, pp. 1474–1478.

[11] M. Elsied, A. Oukaour, H. Gualous, R. Hassan, and A. Amin, "An advanced energy management of microgrid system based on genetic algorithm," in *Proc. IEEE 23rd Int. Symp. Ind. Electron. (ISIE)*, Jun. 2014, pp. 2541–2547.

[12] K. Wang, H. Li, S. Maharjan, Y. Zhang, and S. Guo, "Green energy scheduling for demand side management in the smart grid," *IEEE Trans. Green Commun. Netw.*, vol. 2, no. 2, pp. 596–611, Jun. 2018.

[13] Y. Liu *et al.*, "Distributed robust energy management of a multimicrogrid system in the real-time energy market," *IEEE Trans. Sustain. Energy*, vol. 10, no. 1, pp. 396–406, Jan. 2019.

[14] A. T. Eseye, D. Zheng, J. Zhang, and D. Wei, "Optimal energy management strategy for an isolated industrial microgrid using a modified particle swarm optimization," in *Proc. IEEE Int. Conf. Power Renew. Energy (ICPRE)*, Oct. 2016, pp. 494–498.

[15] S. A. Pourmousavi, H. Nehrir, C. Colson, and C. Wang, "Real-time energy management of a stand-alone hybrid wind-microturbine energy system using particle swarm optimization," in *Proc. IEEE Power Energy Soc. Gen. Meeting*, Jul. 2011, p. 1.

[16] C. M. Colson, M. H. Nehrir, and C. Wang, "Ant colony optimization for microgrid multi-objective power management," in *Proc. IEEE/PES Power Syst. Conf. Expo.*, Mar. 2009, pp. 1–7.

[17] B. Papari, C. S. Edrington, T. V. Vu, and F. Diaz-Franco, "A heuristic method for optimal energy management of DC microgrid," in *Proc. IEEE 2nd Int. Conf. DC Microgrids (ICDCM)*, Jun. 2017, pp. 337–343.

[18] B. Papari, C. S. Edrington, I. Bhattacharya, and G. Radman, "Effective energy management of hybrid AC-DC microgrids with storage devices," *IEEE Trans. Smart Grid*, vol. 10, no. 1, pp. 193–203, Jan. 2019.

[19] P.-A. Jaboulay, W. Zhu, X. Niu, X. Pan, and S. Gao, "Real-time energy management optimization using model predictive control on a microgrid demonstrator," in *Proc. IEEE Int. Conf. Energy Internet (ICEI)*, Apr. 2017, pp. 226–231.

[20] T. Morstyn, B. Hredzak, R. P. Aguilera, and V. G. Agelidis, "Model predictive control for distributed microgrid battery energy storage systems," *IEEE Trans. Control Syst. Technol.*, vol. 26, no. 3, pp. 1107–1114, May 2018.

[21] T. V. Vu, S. Paran, F. Diaz, T. E. Meyzani, and C. S. Edrington, "Model predictive control for power control in islanded DC microgrids," in *Proc. 41st Annu. Conf. IEEE Ind. Electron. Soc. (IECON)*, Nov. 2015, pp. 1610–1615.

[22] Z. Wang, B. Chen, J. Wang, M. M. Begovic, and C. Chen, "Coordinated energy management of networked microgrids in distribution systems," *IEEE Trans. Smart Grid*, vol. 6, no. 1, pp. 45–53, Jan. 2015.

[23] Y. Xiang, J. Liu, and Y. Liu, "Robust energy management of microgrid with uncertain renewable generation and load," *IEEE Trans. Smart Grid*, vol. 7, no. 2, pp. 1034–1043, Mar. 2016.

[24] J. Wu, X. Xing, X. Liu, J. M. Guerrero, and Z. Chen, "Energy management strategy for grid-tied microgrids considering the energy storage efficiency," *IEEE Trans. Ind. Electron.*, vol. 65, no. 12, pp. 9539–9549, Dec. 2018.

[25] N. Gupta *et al.*, "Cost optimal control of microgrids having solar power and energy storage," in *Proc. IEEE/PES Transmiss. Distrib. Conf. Expo. (T&D)*, Apr. 2018, pp. 1–9.

[26] P. Kotsampopoulos *et al.*, "A benchmark system for hardware-in-the-loop testing of distributed energy resources," *IEEE Power Energy Technol. Syst. J.*, vol. 5, no. 3, pp. 94–103, Sep. 2018.

[27] D. D. Dunlap, C. V. Caldwell, E. G. Collins, and O. Chuy, *Motion Planning for Mobile Robots via Sampling-Based Model Predictive Optimization*, A. V. Topolov, Ed. Rijeka, Croatia: InTech, 2012.

[28] B. M. Reese and E. G. Collins, "A graph search and neural network approach to adaptive nonlinear model predictive control," *Eng. Appl. Artif. Intell.*, vol. 55, pp. 250–268, Oct. 2016.

[29] J. H. Halton, "On the efficiency of certain quasi-random sequences of points in evaluating multi-dimensional integrals," *Numerische Math.*, vol. 2, no. 1, pp. 84–90, 1960.

[30] P. E. Hart, N. J. Nilsson, and B. Raphael, "A formal basis for the heuristic determination of minimum cost paths," *IEEE Trans. Syst. Sci. Cybern.*, vol. SSC-4, no. 2, pp. 100–107, Jul. 1968.

[31] J. Ospina, A. Newaz, and M. O. Faruque, "Forecasting of PV plant output using hybrid wavelet-based LSTM-DNN structure model," *IET Renew. Power Gener.*, vol. 13, no. 7, pp. 1087–1095, 2019.

[32] R. Meeker *et al.*, "High penetration solar PV deployment sunshine state solar grid initiative (SUNGRIN)," Florida State Univ., Tallahassee, FL, USA, Final Rep. DOE-FSU-04682-1, 2015.

[33] J. Zhang, B.-M. Hodge, A. Florita, S. Lu, H. Hamann, and V. Banunarayanan, "Metrics for evaluating the accuracy of solar power forecasting," Nat. Renew. Energy Lab., Golden, CO, USA, Tech. Rep. NREL/CP-5000-60142, 2013.

[34] J.-K. Eom, S.-R. Lee, E.-J. Ha, B.-Y. Choi, and C.-Y. Won, "Economic dispatch algorithm considering battery degradation characteristic of energy storage system with PV system," in *Proc. 17th Int. Conf. Elect. Mach. Syst. (ICEMS)*, Oct. 2014, pp. 849–854.

[35] O. Tremblay and L.-A. Dessaint, "Experimental validation of a battery dynamic model for EV applications," *World Electr. Veh. J.*, vol. 3, pp. 1–10, May 2009.